2022

Examining the Effects of Synthetic Dye Yellow No. 5 (Tartrazine) Exposure on Mouse Neuro2A Neurons In Vitro

Jenna L. Farnum
University of Central Florida

EXAMINING THE EFFECTS OF SYNTHETIC DYE YELLOW NO. 5 (TARTRAZINE) EXPOSURE ON MOUSE NEURO2A NEURONS *IN VITRO*

by
JENNA FARNUM

A thesis submitted in partial fulfillment of the requirements for the
Honors in the Major program in Biomedical Sciences
in the College of Medicine
and in the Burnett Honors College
at the University of Central Florida.
Orlando, FL

Spring Term 2022

Thesis Chair: Dr. Alicia Hawthorne, Ph.D.

ABSTRACT

Yellow Dye No. 5, also known as tartrazine (TRZ), is widely used[1] and has an accepted daily intake (ADI) of 0-7.5 mg/kg of body weight per day[2]. Consuming TRZ dosages greater than the ADI can lead to reduced levels of antioxidant enzymes in the brain, chromosomal alterations, or neuronal dendritic changes, [3, 4] which can result in oxidative stress, impaired neuronal functioning and potential mutagenic effects. Within the ADI, there have been observed reductions of the copper zinc superoxide dismutase-1 (SOD1) enzyme levels.[5] We hypothesize that TRZ interacts pre-translationally inside the cell, resulting in the reduction of SOD1 mRNA. In this study, differentiated Neuro2A-derived neurons were exposed to TRZ for 3 or 7 days. We tested a concentration curve from 0 to 11 μg/mL. Treated cells were grown on poly-L-lysine (PLL)- and laminin-coated glass coverslips, immunostained with anti-β-tubulin III and phalloidin, imaged, and analyzed using NeuronJ/ImageJ (NIH). Neurons were traced to analyze the morphological impacts of TRZ. SOD1 mRNA was quantified using reverse transcription quantitative polymerase chain reaction (RT-qPCR). We analyzed the differences in SOD1 mRNA levels of the controls vs. experimental cells, using the $2^{-\Delta\Delta CT}$ statistical method. We found that TRZ caused an increase in neurite length and a general decreasing trend of SOD1 mRNA expression. The reduction in SOD1 mRNA expression could indicate possible pre-translational modifications, which could be a result of TRZ's ability to bind DNA. These findings help fill the gap in understanding the mechanism of SOD1 downregulation due to TRZ exposure.

ACKNOWLEDGEMENTS

I would like to extend my thanks and appreciation to Isadore Nottolini and Colten Frank for their help and support throughout this project. I would like to thank Dr. Emily Bradshaw and Nicole Verity for their assistance and being a part of my thesis committee. I would also like to thank Dr. Stephen King for his advice, resources and participation on my thesis committee. I would like to thank my friends and family for their support and encouragement throughout this project. Lastly, I would like to recognize and extend my deepest gratitude to my thesis chair, Dr. Alicia Hawthorne, for providing me with vital guidance and being an exceptional mentor.

TABLE OF CONTENTS

ABSTRACT II

ACKNOWLEDGEMENTS III

LIST OF TABLES V

LIST OF FIGURES VI

LIST OF ABBREVIATIONS VII

INTRODUCTION 1

1. Tartrazine 1
2. Oxidative Stress 8
3. Superoxide Dismutase 9

METHODS 12

1. Neuro2A cells 12
2. Experimental Conditions 12
3. Immunostaining 13
4. Reverse Transcription Quantitative Polymerase Chain Reaction 14

RESULTS 16

1. Immunostaining 16
2. RT-qPCR 19

DISCUSSION 21

REFERENCES 24

LIST OF TABLES

Table 1: qPCR Primers..... 14

LIST OF FIGURES

Figure 1: Tartrazine Chemical Structure..... 2
Figure 2: Metabolic Breakdown of TRZ..... 7
Figure 3: The Fenton Reaction..... 8
Figure 4: Hypothesis Figure..... 11
Figure 5: Diagram of Experimental Methods 15
Figure 6: Mouse Neuro2a Neuronal Cell Morphology After TRZ Treatment. 17
Figure 7: TRZ Dose Response Curve of SOD1 mRNA Expression 19

LIST OF ABBREVIATIONS

TRZ—Tartrazine

ADI—Accepted daily intake

B.W.—Body Weight

SOD—Superoxide Dismutase

FDA—Food and Drug Administration

ROS—Reactive Oxygen species

DMEM—Dulbecco's modified eagle serum

HBSS—Hanks balanced salt

CCFA—Forty-seventh Session of Codex Committee on Food Additives

INTRODUCTION

1. Tartrazine

Tartrazine (TRZ) was discovered by German chemist Johann Herinrich Ziegler in 1884 while studying what materials could be derived from coal tar [6]. TRZ is currently used as a synthetic yellow dye for materials like wool, food products and cosmetics [7]. The chemical name for TRZ is trisodium 5-hydroxy-1-(4-sulfonatophenyl)-4-(4-sulfonatophenylazo)-H-pyrazol-3-carboxylate, also commonly referred to as FD&C Yellow No. 5 [8]. The chemical structure of TRZ is illustrated In Figure 1. TRZ is classified as an azo dye due to the presence of the azo group (N=N) and has a molecular weight of 534.4 g/mol [9]. The use of artificial food dyes in the United States has increased more throughout recent years, however, food coloring has been a part of the human culture since 1500 B.C. according to Ancient Egyptian writings [3]. These writings indicated that food coloring became a criterion for selecting food products[3]. The Food and Drug Administration (FDA) set the accepted daily intake (ADI) of TRZ to 0-7.5 mg per kilogram of body weight [10]. This ADI has gone under review several times after new findings from studies conducted by the Food and Agriculture Organization (FAO) and the World Health Organization (WHO) illustrating a link between TRZ consumption and hyperactivity in human experiments[2]. The most recent reevaluation was at the 82nd meeting of the Joint FAO/WHO Expert Committee on Food Additives (JECFA) [2]. During this evaluation, the committee concluded that the ADI remain the same after reviewing the current literature and determining that there was a lack of histological and long-term findings [2]. There is also a limit on the

concentration of TRZ allowed into food products, which was set by the WHO and FAO at 50 milligrams per kilogram of food product [11].

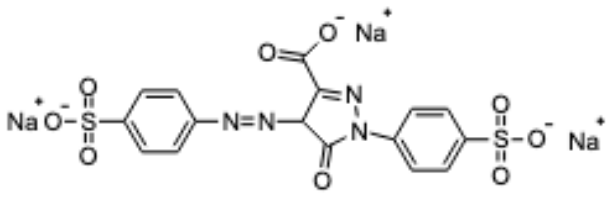

Figure 1: Tartrazine Chemical Structure.

TRZ is commonly found in brightly colored food products, including but not limited to candy, chips, sodas and even some vitamins [1]. Children are more likely to consume higher amounts of TRZ, because it is found in 20.5% of food products targeted towards children[12]. Due to the lower body weight of children compared to that of adults, the actual daily intake of TRZ for children is higher than adults[13]. However, monitoring the correct and accurate TRZ intake level among children can be difficult. In another study that was able to measure the TRZ intake of school-aged children, researchers found that TRZ was found in 42.3% of the food products consumed by the children [14]. Despite set ADI and food concentration limits of TRZ, people are still at risk for consuming large amounts of TRZ-containing products and are susceptible to the potential negative health consequences.

The first concerns regarding the consumption of TRZ were raised in the 1970's after reports of behavioral changes in children that had consumed TRZ. These behavioral changes resembled attention-deficit hyperactivity disorder symptoms, like irritability and restlessness [15]. In 1984, Schauss et al. proposed a link between the consumption of artificial food additives and behavioral issues [16]. TRZ has also been reported to cause

urticaria and asthma in certain individuals, especially in children [1]. In a double-blind study from 1994, Rowe et al. found that after treating children with six experimental dosages (1, 2, 5, 10, 20, 50 mg TRZ), children who were clear reactors displayed irritability, restlessness and sleep disturbance [15]. They also observed that the adverse reactions displayed a dose-response effect and the greater the dosage, the more prolonged the effects were [15]. Ward (1997) observed that, after consuming TRZ-containing drinks, children had increased levels of hyperactivity, increased aggression and had either developed eczema and/or asthma [17]. These results contributed to the Forty-seventh Session of Codex Committee on Food Additives (CCFA) requesting the reevalution of TRZ and further signaled researchers to confirm these results [2].

Outside of the ADI range, there are many reports of observable adverse reactions to tartrazine administration *in vivo* [18-27]and *in vitro* [28-30] . For example, in a study treating fibroblast cells with 5-20 μg/mL of TRZ, researchers found there was a significantly higher percentage of chromosomal aberrations in the experimental group than the control [24]. TRZ in dosages of 20, 500 or 2000 mg/kg of body weight administered to male mice caused increased DNA damage in a dose-dependent manner [25]. In a prenatal study involving TRZ exposure in female rats, researchers observed that affected offspring had altered glutamatergic signaling within the hippocampus [26]. Gao et al. treated mice with 350 mg/kg of TRZ for 30 days [8]. The treated mice exhibited a significant increase in escape latency in the water maze test [8]. This indicated a possible link between chronic consumption of TRZ and impairment of learning and memory of mice [8]. In a recent assessment conducted by the Office of Environmental Health Hazard, researchers

discovered a total of 27 human studies in which TRZ was administered in dosages of 1-125 mg/kg of body weight per day [27]. Out of these studies, researchers noticed a consistent result of hyperactivity even in dosages that fall within the ADI range [27]. However, there have also been some TRZ assessment studies that have found no adverse effects from very large dosages of TRZ. For example, Borzelleca et al. found that rats treated with 2641-3348 mg/kg of TRZ displayed no harmful effects [31]. The restrictions of TRZ concentration in food products, suggested ADI, and the abundance of literature highlights the potential negative health effects of consuming TRZ in dosages greater than the ADI.

Within the ADI there have been reports of adverse reactions to TRZ consumption [5, 7, 19, 20, 28, 30, 32-38]. Himri et al. treated Wistar rats with TRZ in dosages of 5, 7.5 or 10 mg/kg b.w. for a period of 90 days [38]. Compared to the control group, TRZ treated rats did not display any changes in food intake, mortality or body weight. However, there were significant decreases in the weight of the kidneys and increase in weight of the liver. In addition, rats treated with 7.5 mg/kg b.w. of TRZ displayed significantly lower blood platelet count [38]. Himri et al. also noted that red blood cells (RBCs) of the TRZ-treated rats displayed morphological changes from a discoid shape to a echinocytic shape and these changes were observed in a dose-dependent manner [38]. Abd-Elhakim et al. treated rats with 1.35 mg/kg TRZ for a duration of 90 days and analyzed the impacts it had on certain hematological parameters, tissues and expression levels of a few interleukin genes [7]. Their results showed that TRZ-treated rats displayed increased white blood cell levels, necrosis of splenic tissues, and increased expression of interleukin genes [7]. They also noted significant exhaustion of the TRZ-treated rats' innate immune system, based on

decreased lysozymal and phagocytic activity [7]. Albasher et al. treated pregnant female mice with either 2.5 or 5 mg/kg TRZ for a period of 35 days to determine the consequences of prenatal exposure to TRZ [5]. The offspring of the TRZ-treated groups displayed cerebral neuronal degeneration, whereas the control offspring had normal histological findings [5]. Albasher et al. also discovered that both dosages of TRZ-induced lipid peroxidation and suppression of antioxidants in the studied brain regions of the mice offspring, in a dose-dependent manner [5]. Wopara et al. treated rats with TRZ dosages of 2.5, 5, 10 or 20 mg/kg for 23 days and then measured reproductive hormone levels, gene expression of pro-inflammatory cytokines and testicular genes, and histology of the testes [19]. They found that there were significant increases in the follicle stimulating hormone (FSH), luteinizing hormone (LH) and testosterone for all dosages [19]. Wu et al. wanted to understand the impacts TRZ consumption had on antioxidant enzyme levels in crucian carp. Using TRZ dosages of 1.4, 5.5 and 10 mg/kg, they found that at both 5.5 and 10 mg/kg there was triggered oxidative stress, which was indicated by the increase in malondialdehyde (MDA) levels [20]. The occurrence of oxidative stress could have been caused by the reported reduction of superoxide dismutase (SOD) and glutathione peroxidase (GSH-Px) [39]. Another related study aimed to further understand the mechanism by which TRZ induces oxidative and neuroinflammatory damage by treating lymphocytes with TRZ concentrations of 0.25, 0.5, 1.0, 2,0, 4.0, 8.0, 16.0 and 32.0 mM [40]. Soares et al. found that after just 3 hours of exposure, there was new DNA damage at all dosages and with repeated treatment found higher incidences of damage [40].

There have been additional reports of the genotoxic effects of TRZ consumption. For example, Nasri et al. discovered that TRZ is a synthetic xenoestrogen and therefore can activate estrogen receptors *in vitro* [30]. This can lead to potentially hazardous activation or inhibition of estrogen pathways. Due to reports of inflammation after TRZ consumption, Raposa et al. investigated the expression levels of common inflammatory markers NFκB, GADD45α and MAPκ8 [41]. They found that TRZ was able to increase expression of both NFκB and MAPκ8 [41]. Kashanian et al. studied the DNA-binding ability of TRZ using calf thymus DNA and techniques like ultraviolet-visible spectroscopy and circular dichroism [42]. Their findings illustrated that TRZ exhibited competitive binding with the DNA stain Hoechst 33258 and that it binds to DNA within the minor groove [42]. In addition, the binding of TRZ induced a conformation change of the DNA from B-like to C-like and the binding was entropically driven [42]. Mpountoukas et al. studied the genotoxic effects of TRZ on human peripheral blood cells and found that concentrations of 4 and 8 mM had a significant effect on the condensation of chromosomes during mitosis [3]. Soares et al. also discovered tartrazine's ability to strongly bind to linear double-stranded DNA [40]. However, a study by Elhkim et al. found that TRZ has no mutagenic potential *in vivo* or *in vitro* [13]. Due to the conflicting studies regarding the potential genotoxic effects of TRZ,

further investigation into these mechanisms is required to evaluate the safety of TRZ consumption.

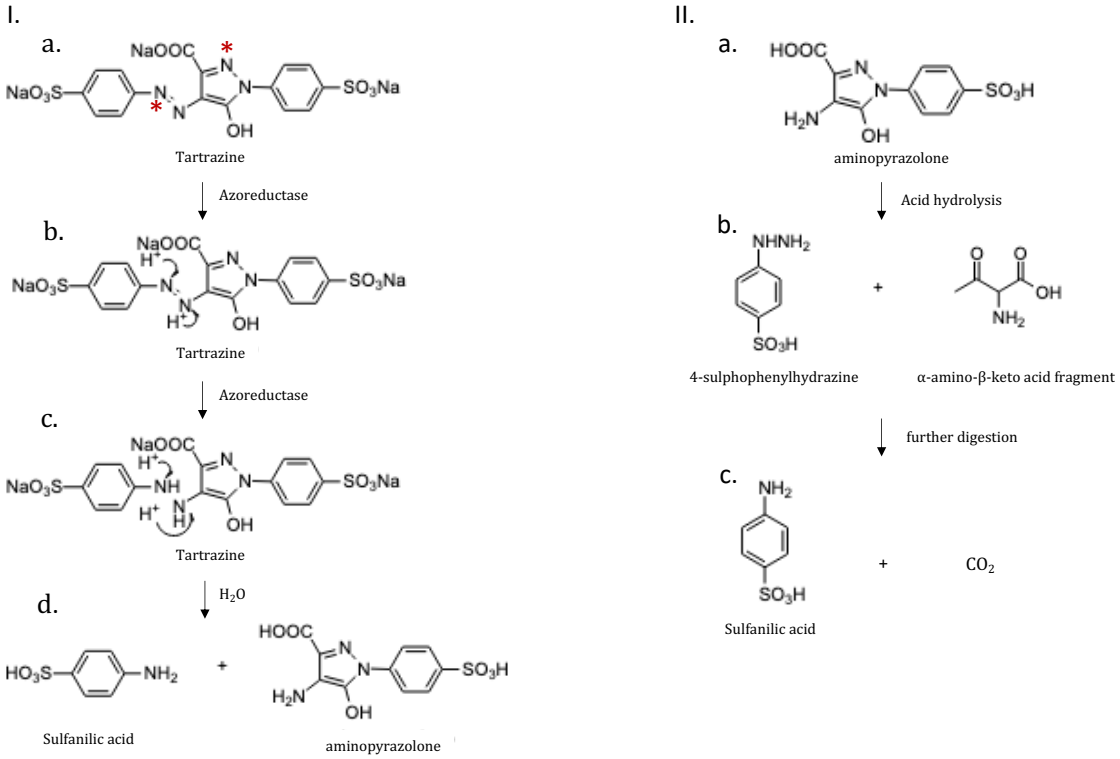

Figure 2: Metabolic Breakdown of TRZ. Upon consumption TRZ is broken down via azoreductase, an enzyme produced by gut microflora (I. a-b)[43]. Products produced in steps II. a-c are all capable of being broken down into ammonia, with the exception of CO_2, and can contribute to the formation of reactive oxygen species [43]. * = sites susceptible to reduction.

Toxicokinetic studies have illustrated that around 2% of TRZ is absorbed directly into the blood stream, while the remaining TRZ is reduced by intestinal microflora [43]. As observed in Figure 2, there are many reduction sites within the chemical structure of TRZ (marked by *). The most susceptible site is the azo bond (N=N), which the stability of this bond depends on the level of reductive agents [38]. Breakdown of TRZ via reduction will lead to formation of different kinds of amines (aniline, sulfanilic acid, etc.), which can be further reduced to form ammonia [38]. Sulfanilic acid and an aminopyrazolone are

common aromatic amines produced as a result of tartrazine digestion, these products are found in urine at ranges from 38-67% of the consumed dosage [44]. These metabolites can lead to the production of reactive oxygen species (ROS), which brings risk of oxidative stress.

2. Oxidative Stress

Figure 3: The Fenton Reaction. This pathway illustrates one mechanism by which the superoxide ion (O_2^-) can be converted into H_2O via antioxidant enzymes superoxide dismutase (SOD) and catalase.

Reactive oxygen species (ROS) are molecules that are made from living organisms as a result of metabolism, mitochondrial electron transport and environmental conditions. These molecules are very reactive and therefore can cause damage to proteins, DNA and other cell structures[45]. ROS are also known as free radicals and some of the most common forms consist of superoxide radicals, hydroxyl radicals and hydrogen peroxide. When maintained at healthy levels, ROS can help facilitate necessary mechanisms inside of the cell. Antioxidant enzymes function to maintain a healthy balance of ROS to antioxidant enzymes and whenever that balance favors the ROS, it is termed oxidative stress [46]. While these radicals can be produced by normal cell functioning, they can also be produced as a result of inflammation or exposure to a toxin [46]. As illustrated in Fig. 3, the Fenton Reaction is the path by which ROS are formed and eliminated via antioxidant enzymes like superoxide dismutase and catalase.

Oxidative stress can induce lipid peroxidation, which is defined as the oxidative degradation of the lipids inside of the cell by the excess free radicals [47]. Oxidation of the lipids inside of the cell can increase the permeability of the plasma membrane, which is dangerous for the cell [46]. Overall, oxidative stress can be the cause of a variety of different health conditions, like neurological disorders, cancer, heart and lung conditions [45].

3. Superoxide Dismutase

Antioxidants and antioxidant enzymes are molecules and proteins that help control the levels of ROS. Superoxide dismutase (SOD) is an antioxidant enzyme that takes the superoxide anion and converts it into hydrogen peroxide and an oxygen atom [48], as observed in Fig. 3. SOD is also one of the antioxidant enzymes that has been reportedly reduced as a result of TRZ exposure in both *in vitro* and *in vivo* models.

SOD is activated by the PI3-K (phosphatidylinositol 3-kinase)/AKT (protein kinase B) signal transduction pathway in order to prevent any potential DNA damage from oxidative stress [49]. Mutations within the regions of DNA coding for SOD enzymes or that cause inhibition of the enzyme contribute to health conditions like lung and lymphatic cancer or neurodegenerative diseases like Parkinson's [48]. Mutations in the SOD1 protein are also associated with the development of Amyotrophic lateral sclerosis (ALS) [50]. ALS is a lethal disease that is marked by its progressive degenerative effects on motor neurons [51]. Mutations in this protein associated with ALS cause progressive loss of neurons in the brainstem, upper motor cortex and spinal cord as a result of increased oxidative stress[52].

There are several different forms of SOD enzymes across different species and within the same organisms [53]. For eukaryotic cells, the three main kinds of SOD proteins

are the copper, zinc-SOD1 (cu,zn-SOD1) found in the cytosol and mitochondria, manganese SOD2 (Mn-SOD2) found in the mitochondria, and SOD3 found extracellularly [54]. The Copper and zinc molecules of the CuZn-SOD1 are responsible for catalyzing the reaction of superoxide to hydrogen peroxide, which is then to be eliminated by catalase [55]. Superoxide is the most abundant radical that can be found in the body, therefore, the SOD1 enzyme is the most abundant antioxidant in the body as a result [56].

Multiple sources have reported results indicating that TRZ exposure causes a reduction in the enzymatic activity of the SOD1 enzyme in mouse and rat animal models [5, 8, 21, 22]. The mechanism causing this reduction is still not understood. One possible mechanism could act at the enzyme inhibition level, as TRZ possesses zinc-chelating properties that reduce zinc [55]. Since zinc is partly responsible for SOD1 to convert superoxide to hydrogen peroxide, the reduction of zinc could explain potential enzymatic inhibition by TRZ. It is also possible to control the levels of SOD1 at the chromosomal level. Epigenetic modifications at the promotor of SOD1 genes reduces the levels of the SOD1 enzyme [56].

If SOD1 levels are decreased after TRZ exposure, the current research suggests that the reduction could be a result of pre- or post- translational modifications [55, 56]. Pre-translational modifications could be explained by the ability of TRZ to bind to DNA and induce conformational changes that cause the region of genetic information coding for SOD1 to become inactive or inaccessible. A possible post-translational mechanism of modification could be explained by an inhibitory reaction between the TRZ molecule and the mature SOD1 enzyme. The purpose of this research is to help understand the

intracellular interactions of TRZ with the SOD1 pathway and whether the observed SOD1 reduction occurs pre-translationally or post-translationally. In this study, we designed a protocol to quantify the mRNA expression levels of the mouse SOD1 enzyme with and without TRZ.

Figure 4: Hypothesis Figure. We hypothesize that TRZ will act pre-translationally in the cell and cause a reduction in SOD1 mRNA as well as decreased neurite outgrowth.

METHODS

1. Neuro2A cells

Neuro2A cells are a mouse neuroblastoma-derived cell line (Sigma). Cells were grown in Dulbecco's modified Eagle serum (DMEM; Fisher Scientific) with 10% fetal bovine serum (Fisher Scientific) and 1% penicillin and streptomycin (Fisher Scientific) until reaching about 80% confluency. The differentiation media was composed of neurobasal-A media (Fisher), B-27 supplement (Fisher), 1% glutaMAX (Fisher), 1% penicillin and streptomycin, TRZ and 12.5 μM forskolin (Sigma). Cells were maintained in a humidified incubator at 37°C and 5% CO_2.

2. Experimental Conditions

Analytical grade Tartrazine (>99% purity) was purchased from (Sigma). TRZ was prepared by dissolving TRZ powder (0.9375 mg/mL) into Hank's balanced salt solution (HBSS; Fisher) and sterile filtered. TRZ in dosages of 0, 1, 3, 5, 7 and 11 μg/mL were administered to the cells through changing the media.

Coverslips were sterilized in 70% ethanol for 15 minutes, washed three times with sterile water and then treated with 10 mM Poly-L-lysine (Sigma) for 2-hours at 37°C then, 4 μg/mL of Laminin overnight at 37°C (Fisher). For treatment, cells were plated at a density of 39.47 cells/cm^2 into 6 well plates on 25 mm glass coverslips (Fisher) and grown in the differentiation media. The differentiation media contained TRZ at either 0, 1, 3, 5, 7 or 11 μg/mL. At 3DIV, the 3DIV condition mRNA and coverslips were collected and the 7DIV condition's media was changed to fresh differentiation media, with the respective

concentration of TRZ. At 7DIV, the 7DIV condition mRNA and coverslips were then collected.

3. Immunostaining

After the treatment period was over, the media solution was aspirated from each well and a 4% paraformaldehyde fixing solution was added to each coverslip for 15 minutes at room temperature. Coverslips were then washed three times with 10 mM phosphate buffered saline (PBS; Fisher) and placed in a blocking solution for 2 hours at room temperature. The blocking solution was made of 0.1% bovine serum albumin (BSA), 0.1% Triton X-100 (Sigma), 5% normal goat serum (NGS; Fisher), and 10 mM PBS. The primary antibody used was rabbit anti-beta tubulin III (1:200; Invitrogen), which was incubated overnight at 4°C. After primary incubation, the coverslips were washed with 10 mM PBS three times and, before being incubated for 2 hours at room temperature with the secondary antibody goat anti-rabbit Alexa 568 (1:200; Invitrogen). The coverslips were then washed two times quickly with 10 mM PBS and then incubated with Phalloidin Alexa 488 (Fisher) for 30 minutes at room temperature to stain the actin filaments. The coverslips were then washed once with 10 mM PBS and incubated with DAPI for 10 minutes at room temperature to stain the DNA and then washed once in 10 mM PBS.

To view the coverslips, we used the LEICA DMI3000 B inverted fluorescence microscope and the Image-Pro Insight 9 software. We used Image J (NIH) to measure the cell density of each coverslip and Neuron J (NIH) to measure average longest neurite and average neurite length. Our data was statistically analyzed using IBM SPSS. All data was non-parametric. Kruskal-Wallis followed by Mann Whitney *U* test post-hoc were used.

4. Reverse Transcription Quantitative Polymerase Chain Reaction

The mRNA of each condition was collected the RNeasy mini kit (Qiagen) after 3 or 7 DIV. The mRNA was then reverse transcribed into cDNA using the Applied Biosystem's RT buffer and enzyme mix (Applied Biosystems). The mRNA was standardized to the lowest RNA concentration for each trial (< 2µg RNA) before being converted into cDNA in order to compare results of qPCR. The mRNA levels of the SOD1 enzyme and GAPDH (housekeeping gene) were measured using the SsoFast EvaGreen Supermix (Biorad) using the Mini Opticon (Biorad) in 48 well-plates. The primers used were designed using the NIH primer BLAST software and both obtained from IDT and were tested prior to experimentation to check specificity.

Experimental Gene	**Primers**	**Housekeeping Gene**	**Primers**
Mouse SOD1 Forward	3'-ACGGTCCGGTGCAGGGAA-5'	**Mouse GAPDH Forward**	3'-TGACGTGCCGCCTGGAGAAA-5'
Mouse SOD1 Reverse	3'-CTGCACTGGTACAGCCTTGTG-5'	**Mouse GAPDH Reverse**	3'-AGTGTAGCCCAAGATGCCCTTCAG-5'

Table 1: qPCR Primers.

The mRNA expression levels were analyzed using the $2^{-\Delta\Delta CT}$ method to determine the fold difference in expression between each condition. Figure 5 illustrates a flow chart of the experimental methods used for this project.

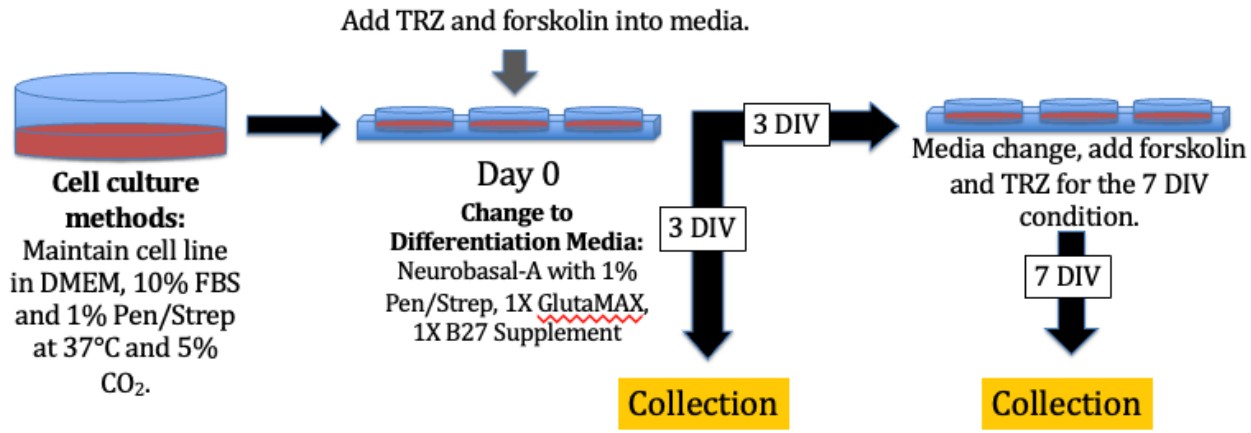

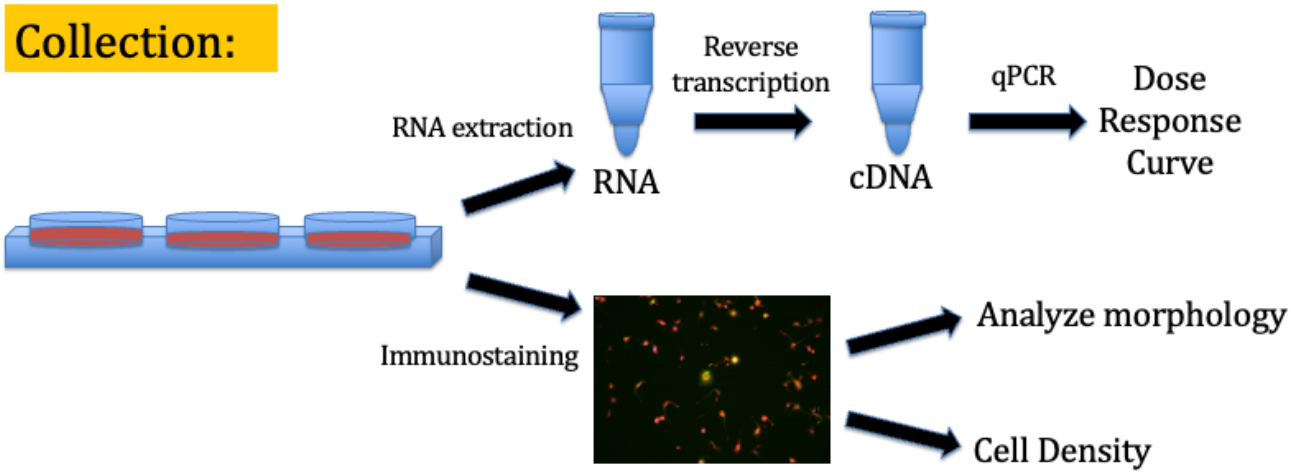

Figure 5: Diagram of Experimental Methods

RESULTS

1. Immunostaining

After the coverslips were stained, they were imaged using fluorescence microscopy. These images were saved and analyzed using the Image J and Neuron J software (NIH) to assess average cell density, average neurite length, average longest neurite and average number of cell branching. The neurites were traced and measured using the Neuron J software. The cell density using DAPI was measured with the Image J counter tool.

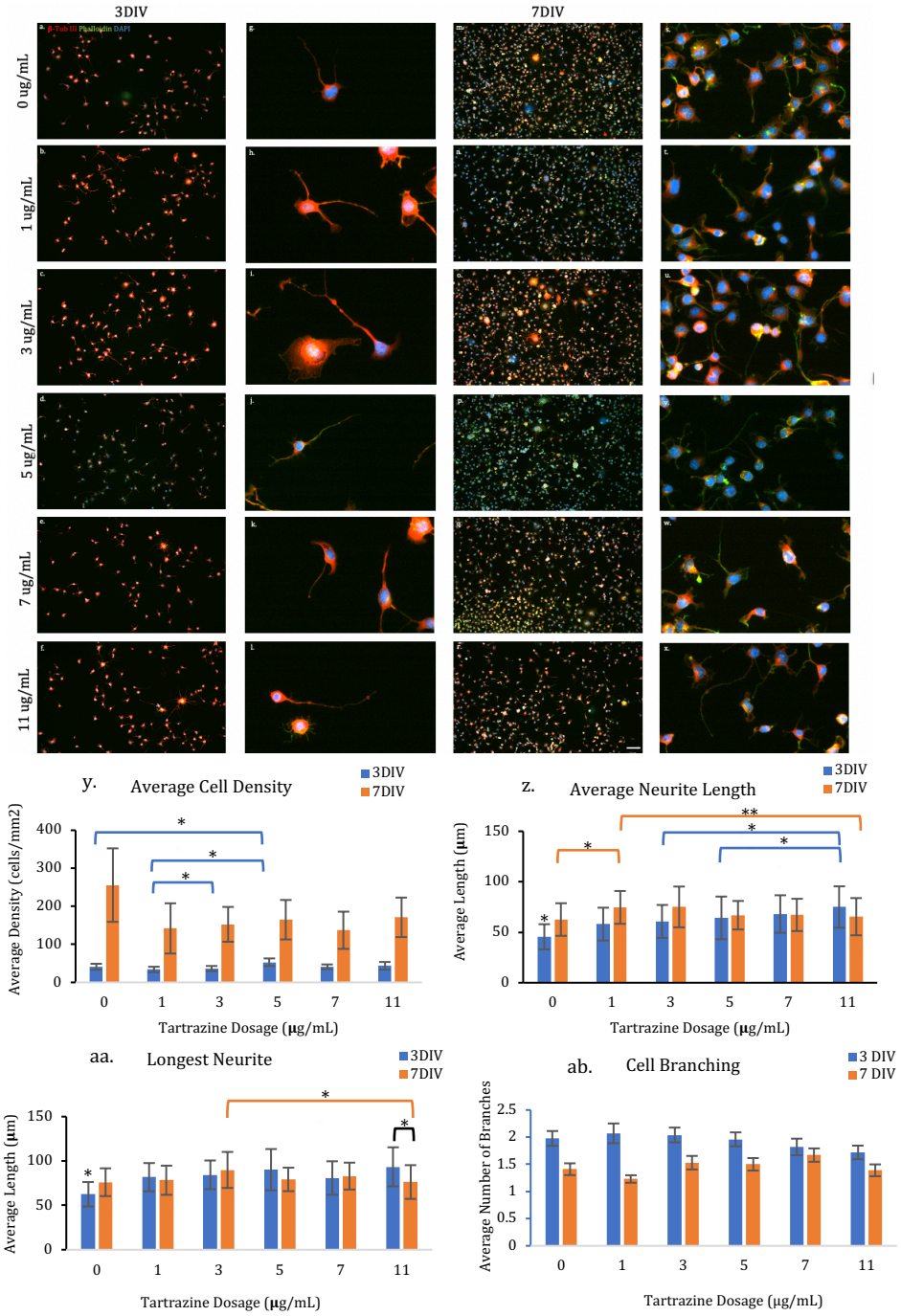

Figure 6: Mouse Neuro2a Neuronal Cell Morphology After TRZ Treatment. Neuro2a cells were imaged after being immunostained for microtubules (red), actin (green) and DNA (blue). Images a-f display cells from the 3DIV condition and images g-l are enlargements of an individual neuron from each condition. Images m-r are examples from the 7DIV condition and images s-x are enlargements of an individual neuron from each dosage. The scale bar is 100 um. Graphs are measurements of cell density (Figure y), average neurite length (Figure z), average longest neurite (Figure aa) and average cell branching (Figure ab). Cell branching at 3DIV is significantly different from 7DIV, indicating more branches at 3DIV than 7DIV ($p < 0.05$).Data was

statistically analyzed with the Kruskal-Wallace test followed by the Mann Whitney U test, *p-value < 0.05, **p-value < 0.01.

The results of average cell density are illustrated in Figure 6y. All the conditions within the 3DIV timepoint were significantly lower in cell density than the 7DIV timepoint dosages with all p-values less than 0.05, except for the 1 μg/mL dose ($p > 0.05$). In addition, within the 3DIV timepoint the 5 μg/mL dose displayed significantly higher cell density than the 0, 1, and 3 μg/mL dosages.

The results for average neurite length are illustrated in Figure 6z. All dosages displayed significantly longer neurite length compared to the 3DIV control, with p-values of less than 0.05. However, within the 3DIV timepoint, there is a significant increase of the 11 μg/mL dose, compared to the 3 and 5 μg/mL dosages with p-values less than 0.05. These results follow the general trend of increasing neurite length with TRZ treatment for the 3DIV condition. For the 7DIV timepoint, there is a significant increase in average neurite length between the 0 and 1 μg/mL dosage with a p-value of 0.022. In addition, there is a significant decrease in neurite length between the 1 and 11 μg/mL dosage of the 7DIV timepoint, with a p-value of 0.018.

The results for the longest neurite length are illustrated in Figure 6aa. The control of the 3DIV timepoint was significantly lower than all other conditions with p-value < 0.05. However, there was a significant decrease in longest neurite length between the 3 μg/mL and 11 μg/mL dose for the 7DIV timepoint. In addition, the 3DIV and 7DIV 11 μg/mL dose were significantly different with all p-values less than 0.05.

The average amount of cell branching (Figure 6ab) only had significant differences between the 3DIV and 7DIV condition with all p-values < 0.05. No other significant differences were present.

2. RT-qPCR

After RNA was extracted from cells and converted into cDNA, the SOD1 mRNA was quantified using qPCR.

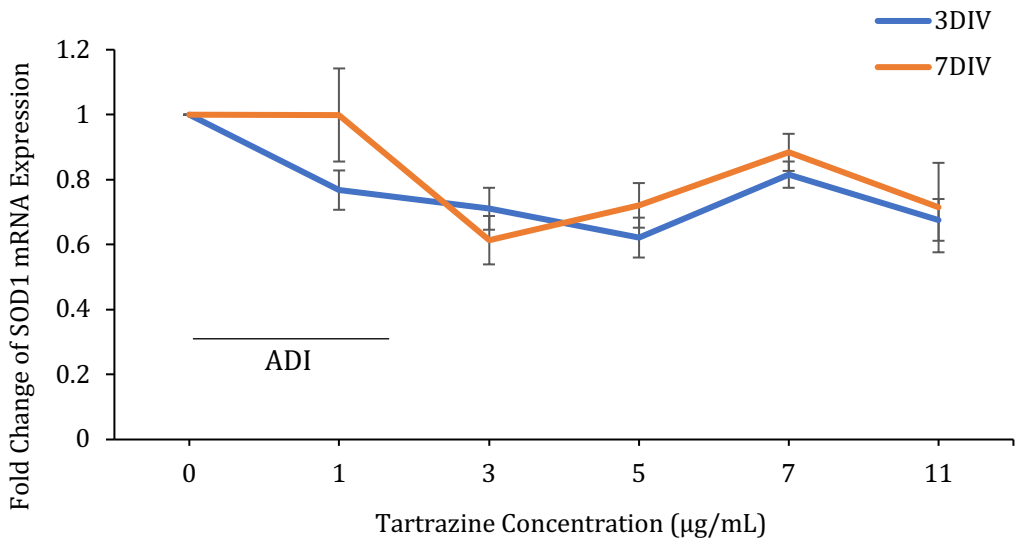

Figure 7: TRZ Dose Response Curve of SOD1 mRNA Expression. The mRNA from each dose and timepoint condition was converted into cDNA. The mRNA levels were compared using the $2^{-\Delta\Delta CT}$ method. GAPDH was used as the housekeeping gene. The ADI for TRZ is 0-1.875 µg/mL. The 7DIV 3 µg/mL condition is significantly lower than the 7DIV 0 and 1 µg/mL condition, with p-values of 0.042 and 0.043, respectively. The statistical tests used were ANOVA ($F(11,36)=3.558$), Tukey post-hoc, *p-value < 0.05.

The results of SOD1 mRNA expression after TRZ treatment are illustrated in Figure 9. There is a significant decrease in SOD1 mRNA expression from the 0 to 3 µg/mL doses of the 7DIV timepoint, with a p-value of 0.042. There is also a significant decrease in expression between the 1 and 3 µg/mL dosage of the 7DIV timepoint, with a p-value of

0.043. These results follow a trend for a reduction in SOD1 mRNA expression after TRZ treatment compared to the control. In addition, at 7DIV the relative fold change of SOD1 mRNA expression resembles a U-shaped graph.

DISCUSSION

Overall, TRZ exposure in mouse neuronal cells leads to an increase in neurite length and reduction in the SOD1 mRNA expression. For the measures of cell density, the significant increase of density found within the 5 μg/mL 3DIV condition resembled a bell-shaped curve that is commonly found in anti-cancer drug resistance [57]. However, these same results were not present within the 7DIV timepoint for cell density. This may point to alternate routes of interaction of TRZ inside the cell.

The results of average neurite length indicated that 0-7 μg/mL TRZ lead to an increase in neurite growth, while 11 μg/mL TRZ in the 7DIV timepoint led to a significant reduction in neurite length. Similar findings were also present within the data of the average longest neurite for each neuron. Rafati et al. [58] found that at a TRZ dosage of 5 mg/kg of b.w. there were significant reductions in time to complete radial maze tests, increased memory errors, and decreased neurite lengths in *in vivo* rat models for a treatment period of 7 weeks. The results of our study may show and early effect of TRZ to increase neurite outgrowth, while a more long-term administration may result in shorter outgrowth. Additional studies including longer timepoints are needed to better understand this mechanism.

For the average amount of cell branching, the only significant differences amongst the results were between the 3DIV and 7DIV conditions. The 3DIV condition had more branching than the 7DIV condition, which is expected as pruning can occur and the neuron can focus on growing longer neurites instead of more neurites [59].

The SOD1 mRNA expression follows a general decreasing trend compared to the control in both the 3DIV and 7DIV timepoints. This reduction is observed in the region in which the calculated ADI for this experiment falls (0-1.875 μg/mL), however is not statistically significant (p-value =0.051). However, there are significant reductions in SOD1 mRNA for dosages greater than the ADI between the 7DIV 0 and 3 μg/mL condition (p-value < 0.05) and the 1 and 3 μg/mL (p-value < 0.05) . This trend for reduction in SOD1 mRNA within the ADI and above the ADI supports the initial hypothesis that TRZ exposure leads to a decrease in SOD1 mRNA expression. The current literature surrounding TRZ exposure and the SOD1 enzyme states that there is a known reduction in the SOD1 enzyme levels [4, 5, 8, 60]. Therefore, the decreasing trend of expression suggests that the reduced protein levels of SOD1 are a result of a pre-translational modification or increased mRNA instability. A possible mechanism of pre-translational modifications caused by TRZ could be explained by TRZ's ability to bind DNA in the minor groove [42]. The DNA binding ability of TRZ could alter the expression of the SOD1 gene, possibly explaining the reductions in SOD1 mRNA and protein levels. In addition, in the 7DIV condition the curve for relative change in SOD1 mRNA expression was similar to a U-shaped graph that is also seen in some anti-cancer drugs. Researchers investigating anti-cancer drugs have noted certain behaviors of resistance with dose-response curves. There are several different mechanisms by which cancer cells can become resistance to anti-cancer drugs. Some of these mechanisms can act via drug inactivation, transporting the drug out of the cell, changing drug metabolism, enhancing DNA repair, gene amplification, epigenetic changes or microRNA (miRNA) interference [61]. Recent research into anti-cancer drugs has revealed patterns of

resistance in the form of U/J-shaped or bell-shaped dose-response graphs. Bell-shaped graphs tend to exhibit stimulation at lower concentrations and inhibition at higher concentrations. Whereas for the U/J-shaped graphs, at low concentrations of the drug there is inhibition of the cancer cells, but there is stimulation at higher concentrations [57].

Due to the variability of significant trends between the 3DIV and 7DIV timepoints, TRZ may have a more noticeable impact within the cell at more short-term treatment periods. Therefore, future directions could implement additional timepoints at shorter increments, as well as more acute dosages. Additionally, additional antioxidant enzymes could be tested to observe if there are similar effects. Future studies could also analyze to which regions of DNA TRZ binds and if this binding is specific or non-specific.

In summation, this research aimed to elucidate whether there are harmful impacts of consuming tartrazine within the accepted daily intake and if the observed reduction of SOD1 levels is due to pre-transcriptional modifications after tartrazine exposure. Utilizing an *in vitro* model with mouse neuronal cells we found that our results may suggest that SOD1 mRNA levels may be altered within the ADI of TRZ and that TRZ treatment had a significant increase in neurite outgrowth within the ADI. These findings can alert people to be cautious of TRZ consumption even at dosages within the ADI in order to avoid adverse reactions like hyperactivity, cancer and neurodegenerative diseases associated with decreased SOD1 activity.

REFERENCES

1. Matsyura, O., et al., *HYPERSENSITIVITY REACTIONS TO FOOD ADDITIVES IN PEDIATRIC PRACTICE: TWO CLINICAL CASES.* Georgian Med News, 2020(307): p. 91-95.
2. (JECFA), J.F.W.E.C.o.F.A., *Safety evaluation of certain food additives*, F.a.A.O.o.t.U. Nations, Editor. 2017, World Health Organization: WHO Food Additive Series. p. 502.
3. Mpountoukas, P., et al., *Cytogenetic evaluation and DNA interaction studies of the food colorants amaranth, erythrosine and tartrazine.* Food Chem Toxicol, 2010. **48**(10): p. 2934-44.
4. Abd-Elhakim, Y.M., et al., *Influence of the long-term exposure to tartrazine and chlorophyll on the fibrogenic signalling pathway in liver and kidney of rats: the expression patterns of collagen 1-α, TGFβ-1, fibronectin, and caspase-3 genes.* Environ Sci Pollut Res Int, 2019. **26**(12): p. 12368-12378.
5. Albasher, G., et al., *Perinatal Exposure to Tartrazine Triggers Oxidative Stress and Neurobehavioral Alterations in Mice Offspring.* Antioxidants (Basel), 2020. **9**(1).
6. Ziegler, J.H. and M. Locher, *Ueber die Tartrazine, eine neue Klasse von Farbstoffen*. 1887: Chemistry Europe.
7. Abd-Elhakim, Y.M., et al., *Comparative haemato-immunotoxic impacts of long-term exposure to tartrazine and chlorophyll in rats.* Int Immunopharmacol, 2018. **63**: p. 145-154.
8. Gao, Y., et al., *Effect of food azo dye tartrazine on learning and memory functions in mice and rats, and the possible mechanisms involved.* J Food Sci, 2011. **76**(6): p. T125-9.
9. Information, N.C.f.B., *PubChem Compound Summary for CID 164825, Tartrazine.* 2021: https://pubchem.ncbi.nlm.nih.gov/compound/Tartrazine.
10. Rosenblatt, D., *Inert Ingredient Tolerance Reassessment - FD&C Blue No. 1, FD&C Red No. 40, and FD&C Yellow No. 5 (Tartrazine)*. 2004, Office of Prevention, Pesticides and Toxic Substances: UNITED STATES ENVIRONMENTAL PROTECTION AGENCY. p. 31.
11. Liu, L., et al., *Development of a highly sensitive fluorescence method for tartrazine determination in food matrices based on carbon dots.* Anal Bioanal Chem, 2021. **413**(5): p. 1485-1492.
12. Batada, A. and M.F. Jacobson, *Prevalence of Artificial Food Colors in Grocery Store Products Marketed to Children.* Clin Pediatr (Phila), 2016. **55**(12): p. 1113-9.
13. Elhkim, M.O., et al., *New considerations regarding the risk assessment on Tartrazine An update toxicological assessment, intolerance reactions and maximum theoretical daily intake in France.* Regul Toxicol Pharmacol, 2007. **47**(3): p. 308-16.
14. Asif Ahmed, M., et al., *Dietary intake of artificial food color additives containing food products by school-going children.* Saudi J Biol Sci, 2021. **28**(1): p. 27-34.
15. Rowe, K.S. and K.J. Rowe, *Synthetic food coloring and behavior: a dose response effect in a double-blind, placebo-controlled, repeated-measures study.* J Pediatr, 1994. **125**(5 Pt 1): p. 691-8.

16. Schauss, A.G., *Nutrition and behavior: complex interdisciplinary research.* Nutr Health, 1984. **3**(1-2): p. 9-37.
17. Ward, N.I., *Assessment of chemical factors in relation to child hyperactivity.* Journal of Nutrition and Environmental Medicine, 1997. **7**: p. 333-342.
18. Wopara, I., et al., *Anxiogenic and memory impairment effect of food color exposure: upregulation of oxido-neuroinflammatory markers and acetyl-cholinestrase activity in the prefrontal cortex and hippocampus.* Heliyon, 2021. **7**(3): p. e06378.
19. Wopara, I., et al., *Synthetic Food dyes cause testicular damage via up-regulation of pro-inflammatory cytokines and down-regulation of FSH-R and TESK-1 gene expression.* JBRA Assist Reprod, 2021. **25**(3): p. 341-348.
20. Wu, L., et al., *Impacts of an azo food dye tartrazine uptake on intestinal barrier, oxidative stress, inflammatory response and intestinal microbiome in crucian carp (Carassius auratus).* Ecotoxicol Environ Saf, 2021. **223**: p. 112551.
21. Alsalman, N., et al., *High-Dose Aspirin Reverses Tartrazine-Induced Cell Growth Dysregulation Independent of p53 Signaling and Antioxidant Mechanisms in Rat Brain.* Biomed Res Int, 2019. **2019**: p. 9096404.
22. Connolly, A., et al., *Pattern of intake of food additives associated with hyperactivity in Irish children and teenagers.* Food Addit Contam Part A Chem Anal Control Expo Risk Assess, 2010. **27**(4): p. 447-56.
23. Gupta, R., et al., *Toxic Effects of Food Colorants Erythrosine and Tartrazine on Zebrafish Embryo Development* Current Research in Nutrition and Food Science Journal, 2019. **7**: p. 876-885.
24. Patterson, R.M. and J.S. Butler, *Tartrazine-induced chromosomal aberrations in mammalian cells.* Food Chem Toxicol, 1982. **20**(4): p. 461-5.
25. Bastaki, M., et al., *Lack of genotoxicity in vivo for food color additive Tartrazine.* Food Chem Toxicol, 2017. **105**: p. 278-284.
26. Doguc, D.K., et al., *Prenatal exposure to artificial food colorings alters NMDA receptor subunit concentrations in rat hippocampus.* Nutr Neurosci, 2019: p. 1-11.
27. Center, C.s.E.H., *Health Effects Assessment: Potential Neurobehavioral Effects of Synthetic Food Dyes in Children*, C.E.P. Agency, Editor. 2020: California Office of Environmental Health Hazard Assessment. p. 310.
28. Ameur, F.Z., et al., *Effect of tartrazine on digestive enzymatic activities: in vivo and in vitro studies.* Toxicol Res, 2020. **36**(2): p. 159-166.
29. Joshi, V. and P. Katti, *Developmental Toxicity Assay for Food Additive Tartrazine Using Zebrafish (Danio rerio) Embryo Cultures.* Int J Toxicol, 2018. **37**(1): p. 38-44.
30. Nasri, A. and R. Pohjanvirta, *In vitro estrogenic, cytotoxic, and genotoxic profiles of the xenoestrogens 8-prenylnaringenine, genistein and tartrazine.* Environ Sci Pollut Res Int, 2021. **28**(22): p. 27988-27997.
31. Borzelleca, J.F. and J.B. Hallagan, *A chronic toxicity/carcinogenicity study of FD & C Yellow No. 5 (tartrazine) in mice.* Food Chem Toxicol, 1988. **26**(3): p. 189-94.

32. Atlı Şekeroğlu, Z., et al., *Effects of tartrazine on proliferation and genetic damage in human lymphocytes.* Toxicol Mech Methods, 2017. **27**(5): p. 370-375.
33. Bhatt, D., et al., *Tartrazine induced neurobiochemical alterations in rat brain sub-regions.* Food Chem Toxicol, 2018. **113**: p. 322-327.
34. El-Desoky, G.E., et al., *Regulatory Role of Nano-Curcumin against Tartrazine-Induced Oxidative Stress, Apoptosis-Related Genes Expression, and Genotoxicity in Rats.* Molecules, 2020. **25**(24).
35. El-Sakhawy, M.A., D.W. Mohamed, and Y.H. Ahmed, *Histological and immunohistochemical evaluation of the effect of tartrazine on the cerebellum, submandibular glands, and kidneys of adult male albino rats.* Environ Sci Pollut Res Int, 2019. **26**(10): p. 9574-9584.
36. Floriano, J.M., et al., *Is tartrazine really safe?* Toxicol Res (Camb), 2018. **7**(6): p. 1128-1134.
37. Hashem, M.M., et al., *Embryotoxic and Teratogenic Effects of Tartrazine in Rats.* Toxicol Res, 2019. **35**(1): p. 75-81.
38. Himri, I., et al., *A 90-DAY ORAL TOXICITY STUDY OF TARTRAZINE, A SYNTHETIC FOOD DYE, IN WISTAR RATS*. 2011: International Journal of Pharmacy and Pharmaceutical Sciences.
39. Li, M., et al., *FD&C Yellow No. 5 (tartrazine) degradation via reactive oxygen species triggered by TiO2 and Au/TiO2 nanoparticles exposed to simulated sunlight.* J Agric Food Chem, 2014. **62**(49): p. 12052-60.
40. Soares, B.M., et al., *Effects on DNA repair in human lymphocytes exposed to the food dye tartrazine yellow.* Anticancer Res, 2015. **35**(3): p. 1465-74.
41. Raposa, B., et al., *Food additives: Sodium benzoate, potassium sorbate, azorubine, and tartrazine modify the expression of NFκB, GADD45α, and MAPK8 genes.* Physiol Int, 2016. **103**(3): p. 334-343.
42. Kashanian, S. and S.H. Zeidali, *DNA binding studies of tartrazine food additive.* DNA Cell Biol, 2011. **30**(7): p. 499-505.
43. Murdoch, R.D., I. Pollock, and S. Naeem, *Tartrazine induced histamine release in vivo in normal subjects.* J R Coll Physicians Lond, 1987. **21**(4): p. 257-61.
44. Ryan, A.J., P.G. Welling, and S.E. Wright, *Further studies on the metabolism of tartrazine and related compounds in the intact rat.* Food Cosmet Toxicol, 1969. **7**(4): p. 287-95.
45. Birben, E., et al., *Oxidative stress and antioxidant defense.* World Allergy Organ J, 2012. **5**(1): p. 9-19.
46. Ghosh, N., et al., *Chapter 4 - Reactive Oxygen Species, Oxidative Damage and Cell Death*. 2018, Academic Press: Immunity and Inflammation in Health and Disease. p. 45-55.
47. Ayala, A., M.F. Muñoz, and S. Argüelles, *Lipid peroxidation: production, metabolism, and signaling mechanisms of malondialdehyde and 4-hydroxy-2-nonenal.* Oxid Med Cell Longev, 2014. **2014**: p. 360438.

48. Azadmanesh, J. and G.E.O. Borgstahl, *A Review of the Catalytic Mechanism of Human Manganese Superoxide Dismutase.* Antioxidants (Basel), 2018. **7**(2).
49. Yu, Q.J. and Y. Yang, *Function of SOD1, SOD2, and PI3K/AKT signaling pathways in the protection of propofol on spinal cord ischemic reperfusion injury in a rabbit model.* Life Sci, 2016. **148**: p. 86-92.
50. Moya, M.V., et al., *Unique molecular features and cellular responses differentiate two populations of motor cortical layer 5b neurons in a preclinical model of ALS.* Cell Rep, 2022. **38**(12): p. 110556.
51. Bette, M., et al., *Therapeutic Treatment of Superoxide Dismutase 1 (G93A) Amyotrophic Lateral Sclerosis Model Mice with Medical Ozone Decelerates Trigeminal Motor Neuron Degeneration, Attenuates Microglial Proliferation, and Preserves Monocyte Levels in Mesenteric Lymph Nodes.* Int J Mol Sci, 2022. **23**(6).
52. Collaborators, G.A.Y.A.C., *The global burden of adolescent and young adult cancer in 2019: a systematic analysis for the Global Burden of Disease Study 2019.* Lancet Oncol, 2021.
53. Kobayashi, Y., et al., *Comparative analysis of seven types of superoxide dismutases for their ability to respond to oxidative stress in Bombyx mori.* Sci Rep, 2019. **9**(1): p. 2170.
54. Li, S., et al., *Disrupting SOD1 activity inhibits cell growth and enhances lipid accumulation in nasopharyngeal carcinoma.* Cell Commun Signal, 2018. **16**(1): p. 28.
55. Visweswaran, B. and G. Krishnamoorthy, *Oxidative Stress by Tartrazine in the Testis of Wistar Rats* IOSR Journal of Pharmacy and Biological Sciences, 2012. **2**(3): p. 44-49.
56. Bafana, A., et al., *Superoxide dismutase: an industrial perspective.* Crit Rev Biotechnol, 2011. **31**(1): p. 65-76.
57. Reynolds, A.R., *Potential relevance of bell-shaped and u-shaped dose-responses for the therapeutic targeting of angiogenesis in cancer.* Dose Response, 2010. **8**(3): p. 253-84.
58. Rafati, A., et al., *Using vitamin E to prevent the impairment in behavioral test, cell loss and dendrite changes in medial prefrontal cortex induced by tartrazine in rats.* Acta Histochem, 2017. **119**(2): p. 172-180.
59. Bellon, A., et al., *Dopamine-induced pruning in monocyte-derived-neuronal-like cells (MDNCs) from patients with schizophrenia.* Mol Psychiatry, 2022.
60. Amin, K.A., *Toxicological and Safety assessment of tartrazine as a synthetic food additive on health biomarkers: A review*, F.S. Al-Shehri, Editor. 2017, Academic Journals: African Journal of Biotechnology. p. 139-149.
61. Mansoori, B., et al., *The Different Mechanisms of Cancer Drug Resistance: A Brief Review.* Adv Pharm Bull, 2017. **7**(3): p. 339-348.